

Curing Copolymerization Kinetics of Styrene with Maleated Castor Oil Glycerides Obtained from Biodiesel-Derived Crude Glycerol

David A. Echeverri,¹ Franklin Jaramillo,² Luis A. Rios¹

¹Grupo Procesos Químicos Industriales, Facultad de Ingeniería, Universidad de Antioquia UdeA, Calle 70 No. 52-21, Medellín, Colombia

²Centro de Investigación, Innovación y Desarrollo de Materiales-CIDEMAT, Universidad de Antioquia UdeA, Calle 70 No.52-21, Medellín, Colombia

Correspondence to: L. A. Rios (E-mail: larios@udea.edu.co or lariospfa@gmail.com)

ABSTRACT: Kinetics of curing of maleated castor oil glycerides with styrene was studied by differential scanning calorimetry and rheology. The resin was synthesized from biodiesel-derived crude glycerol. Curing rates were fitted to several empirical models (autocatalytic model, Kamal's model and a model with vitrification). The three models showed a good fitting with experimental data at conversions lower than 0.55 for temperatures ranging from 30 to 50°C. However, the model that includes vitrification showed a better fitting in the entire range of conversions and the same temperatures. At higher temperatures (50–60°C), some deviations were observed for the three models at low and high conversions. Gel times were obtained from rheological studies and the apparent activation energies were calculated thereof. Gel times were 300–2700 s. The values of apparent activation energy obtained for this castor oil-based copolymer (47.2–52.3 kJ/mol) were within range of commercial unsaturated polyester resins. © 2014 Wiley Periodicals, Inc. *J. Appl. Polym. Sci.* **2015**, *132*, 41344.

KEYWORDS: biopolymers and renewable polymers; radical polymerization; kinetics; rheology; thermosets

Received 8 April 2014; accepted 28 July 2014

DOI: 10.1002/app.41344

INTRODUCTION

Synthetic polymers consume around 4% of the world's oil reserves, whose medium-term supply outlook is uncertain. For these reasons, the search for alternative renewable sources of monomers, such as biomass, is a challenging issue. In this field, the oleochemistry offers a lot of feedstocks such as vegetable oils and their derivatives. The advantages of these raw materials include low price, availability, renewability, and biodegradability.¹ According to the US Department of Energy, vegetable oils are a potential feedstock for polymers because their fatty acid molecules can be modified to serve as polymer building blocks.² Unsaturated natural oils such as linseed and tung oil can be polymerized directly through radical mechanisms.³ Fatty acid chains present in the triglyceride oils act as plasticizers, reducing the stiffness of the materials. In addition, the C=C from the fatty acid chains are not enough reactive in radical polymerization, which is more commonly used than cationic polymerization. For this reason, and in order to obtain rigid materials, several polymerizable functional groups are introduced in the triglyceride structure. These functionalities can be attached

through unsaturations, allylic carbons, ester groups, hydroxyl groups, and α carbons to double bonds.³

In the last decade, several works have been devoted to the modification of triglyceride oils through different routes such as epoxidation-acrylation, alcoholysis-maleinization, and hydroxylation-maleinization.^{4–8} For instance, Can et al. reported the synthesis of soybean oil- and castor oil-based monomers prepared via the malinization of alcoholysis products of the oils with various polyols.⁷ These monomers were copolymerized with styrene affording rigid materials. Properties of the resulting polymers were dependent on the structure of the alcohol used and the content of styrene. Castor oil-based thermosets afforded comparable properties to those of high-performance unsaturated polyester resins. Maleated castor oil glycerides (MACOG) obtained from biodiesel-derived crude glycerol (without purification) were synthesized recently by our group.⁹ Residual alkaline catalysts from the biodiesel process (NaOH) was used as catalysts for the glycerolysis reaction. Crude glycerol has a lower value due to impurities and can be used to obtain mono- and di-glycerides through glycerolysis reaction without prior

Additional Supporting Information may be found in the online version of this article.

© 2014 Wiley Periodicals, Inc.

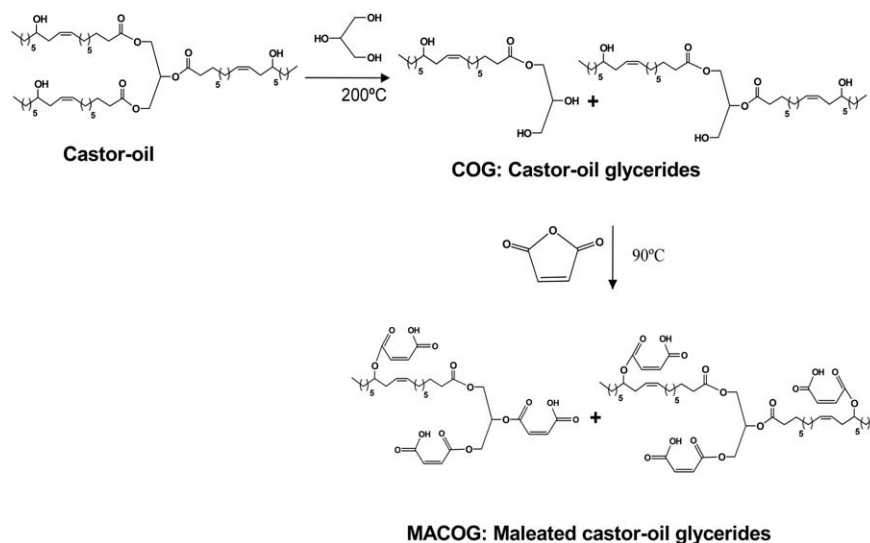


Figure 1. Synthesis of MACOG.

purification.¹⁰ Use of crude glycerol in high added-value applications can improve biodiesel economy.¹¹

Kinetics studies related with the polymerization of maleated glycerides has not been reported before. A deeper understanding of the cure behavior during copolymerization of these resins is essential for commercial applications. Differential scanning calorimetry (DSC) is widely used in the determination of kinetic parameters for curing thermosets. DSC technique measures the rate of heat generated during curing (dQ/dt), which is proportional to relative degree of curing (α).¹² Cure behavior can also be assessed using rheology, where the change in dynamical-mechanical properties of a reacting system is measured as a function of time and temperature. The gel point, which is defined as the time or temperature at which covalent bonds connect irreversible across the network and an infinite network is formed, can be accurately obtained from these measurements.¹²

In this work, the cure kinetics of a copolymer formed between MACOG from biodiesel-derived crude glycerol and styrene was evaluated by DSC and rheology. So far, there are not systematic kinetic studies of curing transition for this copolymer. Commercial initiator-catalyst system consisting of methyl ethyl ketone peroxide (MEKP) and cobalt octoate was used. This is a redox system where Co^{2+} ion promotes decomposition of the organic peroxide producing free radicals.¹³ DSC measurements were conducted under isothermal conditions at several temperatures and initiator concentrations. Kinetic parameters were obtained by fitting of DSC data to empirical models. Gel point was obtained from rheological measurements and apparent activation energies (E_a) were calculated thereof.

EXPERIMENTAL

Materials

Technical grade castor oil (acid value, 1.96 mg KOH/g) was purchased from a local distributor. Methanol ($\geq 99.8\%$), sodium hydroxide ($\geq 97\%$), maleic anhydride ($\geq 99\%$), and styrene

($\geq 99\%$) were purchased from Sigma-Aldrich. MEKP (Butanox-M50) was used as initiator and cobalt octoate (NL51P) as catalyst. These products were donated by AkzoNobel.

Synthesis of Castor Oil Glycerides

Glycerolysis (Figure 1) was carried out in a 250-mL round-bottom flask, equipped with a nitrogen inlet, mechanical stirring, and heating mantle following the procedure of Echeverri et al.⁹ Castor oil (150.0 g) was heated to 200°C and then crude glycerol (42.35 g) were added under stirring. The reaction was completed in 30 min and 2.0 mL of H_2SO_4 solution in water (50% w/w) was added to neutralize the catalyst. The mixture was allowed to cool to 100°C to separate the neutralized catalyst and the most of the excess glycerol in the bottom of the flask.

Crude glycerol was obtained from the transesterification of soybean oil with methanol at 65°C using NaOH as catalyst (0.37 wt % respect to the oil) according to the procedure of Echeverri et al.¹⁰

^1H NMR spectra of the COG showed the following signals [CDCl_3 , δ (ppm)]: 5.54 (m, $-\text{CH}=\text{CH}-\text{CH}_2-\text{CH}(\text{OH})-$), 5.37 (m, $-\text{CH}=\text{CH}-\text{CH}_2-\text{CH}(\text{OH})-$), 5.08 (m, $-\text{CHO}(\text{C}=\text{O})-$), 4.25–4.05 (m, $-\text{CH}_2\text{O}(\text{C}=\text{O})-$), 3.98–3.84 (m, $-\text{CH}-\text{OH}$), 3.76–3.52 (m, CH_2OH), 2.34 (t, $-\text{CH}_2(\text{C}=\text{O})\text{O}-$), 2.20 (m, $\text{CH}-\text{CH}_2-\text{CH}(\text{OH})-$), 2.02 (m, $-\text{CH}_2-\text{CH}=\text{CH}-$), 1.62 (t, $-\text{CH}_2-\text{CH}_2-(\text{C}=\text{O})\text{O}-$), 1.45 (m, $-\text{CH}_2-\text{CH}_2-\text{CH}(\text{OH})-$), 1.42–1.14 (m, $n\text{CH}_2-$), 0.85 (t, CH_3-).

Synthesis of Maleated Castor Oil Glycerides

Maleinization (Figure 1) was carried out in 25-mL round-bottom flask adapted with a condenser according to the procedure of Echeverri et al.⁹ A total of 10.0 g of COG and 15 g of maleic anhydride were added to the flask and the system was introduced in a silicone bath heated at 90°C. The reaction was carried out for 1 h at stirring rate of 350 rpm. The product was washed three times with hot water–NaCl solution to remove the excess of maleic anhydride. Then, the product was dissolved in

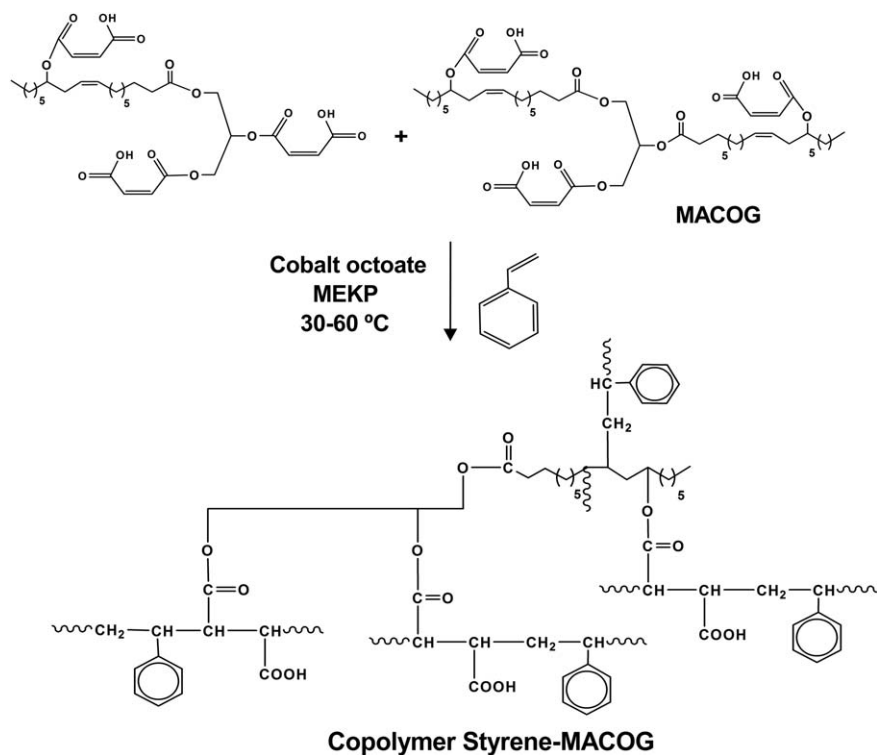


Figure 2. Copolymerization of MACOG-styrene resin. Sluggly lines indicate polystyrene chains.

dichloromethane, dried over anhydrous magnesium sulfate, and filtered. The solvent was evaporated under reduced pressure.

^1H NMR spectra of the product showed the following signals [CDCl_3 , δ (ppm)]: 6.89 (m, $\text{CH}=\text{CH}-$, from fumarate moieties), 6.34 (m, $-\text{OCOCH}=\text{CH}-\text{COOH}$, from maleate moieties), 5.48 (m, $-\text{CHO}(\text{CO})-$), 5.30 (m, $-\text{CH}=\text{CH}$, from fatty acid chain), 5.00 (q, $-\text{CH}=\text{CH}-\text{CH}_2-\text{CHO}(\text{CO})-$), 4.50–4.05 (m, $-\text{CH}_2\text{O}(\text{CO})-$), 2.32 (m, $-\text{CH}_2(\text{CO})\text{O}-$), 2.01 (m, $-\text{CH}_2-\text{CH}=\text{CH}-$), 1.58 (t, $-\text{CH}_2-\text{CH}_2(\text{CO})\text{O}-$), 1.41–1.14 (m, $-\text{CH}_2-$), 0.85 (t, CH_3-).

Kinetic Analysis of MACOG–Styrene Resin Cure

The reaction scheme for the polymerization of MACOG and styrene is showed in Figure 2. Kinetic studies were performed using DSC and rheology. The concentration of styrene was 30 wt % of the total weight of the resin. The concentration of catalyst was 0.5 wt % of the total weight of the resin. The concentrations of MEKP were 0.5, 1.0, and 2.0 wt % of total weight of resin. During DSC analyses MACOG, styrene and catalyst were mixed in a closed vial with magnetic stirring at room temperature. Initiator was added dropwise and the mixture stirred thoroughly. Once MEKP was added, the sample was quickly transferred to DSC for measurements.

The heat released during curing reactions was measured using a TA Instruments Q200 series DSC, under nitrogen. All experiments were performed under isothermal conditions to obtain the heat flow curves. Aluminum capsules with perforated lid were used. The amount of sample used was 12–17 mg in all experiments. Curing was conducted at 30–60°C, according to previous assays. For the isothermal analysis, the DSC cell was allowed to stabilize at each isothermal condition before

introducing the sample. Once isothermal curing was completed, DSC cell was rapidly cooled to room temperature, and when stabilized, the cell was heated at 10°C/min to 200°C until no further exotherm was observed. The exothermic peak generated at last corresponds to the residual heat of curing.

Rheological tests were performed using a Bohlin-Gemini rheometer from Malvern Instruments. The rheometer has disposable aluminum plates in order to track the change in the viscoelastic properties of a thermoset until complete curing or solidification. Aluminum plates (25 mm) in a plate–plate configuration were used. The tests were conducted at a frequency of 1 Hz, and the gap between the plates was 0.5 mm. Assays were conducted at the same temperature conditions of DSC measurements.

Cure Modeling Theory

DSC technique can be used to measure the change in heat flow dQ/dt during isothermal curing of thermosetting resins. It is assumed that the amount of heat generated is proportional to the degree of cure, α at a given time. Therefore, the rate of curing $d\alpha/dt$, can be related to dQ/dt by eq. (1)¹²:

$$\frac{d\alpha}{dt} = \frac{1}{Q_{tot}} \frac{dQ}{dt} \quad (1)$$

by integrating eq. (1), the relative degree of cure can be obtained:

$$\alpha = \frac{1}{Q_{tot}} \int_0^t \left(\frac{dQ}{dt} \right)_T dt \quad (2)$$

the total heat of curing (Q_{tot}) is the sum of the isothermal heat, which is the heat generated during the isothermal DSC test at

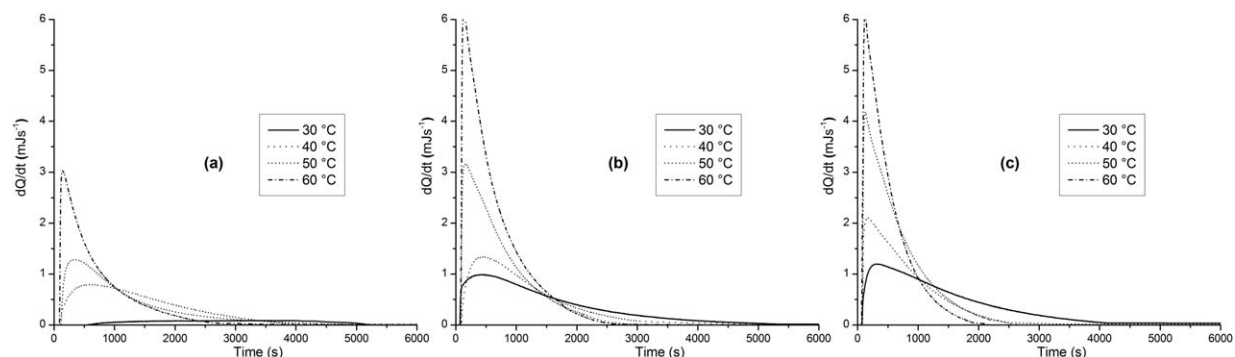


Figure 3. Heat flow versus time for isothermal curing: (a) 0.5 wt % MEKP, (b) 1.0 wt % MEKP, and (c) 2.0 wt % MEKP.

each temperature, and the residual heat, corresponding to the heat released when the sample is heated to a temperature at which curing is completed.¹⁴

The gel time (t_g), measured under isothermal conditions, may be taken as a measure of the overall rate of polymerization of a given system under certain circumstances.¹⁵ E_a values can be obtained also from such measurements. The conversion at the gel point of resin is constant and is not related to the reaction temperature, according to Flory's gelation theory. E_a can be obtained from t_g according to Arrhenius relationship [eq. (3)]:¹⁶

$$\ln(t_g) = \ln A' + \frac{E_a}{R} \cdot \frac{1}{T} \quad (3)$$

where A' is a constant related to the reaction model and R is the universal gas constant.

RESULTS AND DISCUSSION

Synthesis of COG and MACOG

COG were synthesized from castor oil and crude glycerol (without previous purification) during the glycerolysis reaction. No catalyst was added because residual alkaline components (NaOH and soap) from crude glycerol can serve as catalyst of the reaction. On the other hand, COG was esterified with maleic anhydride without catalyst, at 90°C and 1 h, affording a product with 87% conversion of hydroxyl groups. According to Can et al., *N,N*-dimethyl benzylamine is needed for accomplish the maleinization reaction in 5 h and 98°C (affording 85.2% conversion of hydroxyl groups).⁷ In addition, we observed that

use of this catalyst caused darkening of the final resin. MACOG was purified before copolymerization with styrene because some immiscibility was detected once they were mixed. Excess maleic anhydride and glycerol-maleate (formed from remaining glycerol and maleic anhydride) settled from resin.

DSC Cure Characterization

All the experiments were done at 30 wt % styrene and 0.5 wt % Co catalyst. These conditions are used in commercial applications and allow accomplishing the polymerization under practical times. Increasing styrene concentration and/or catalyst concentration increases reaction rate as shown in previous works related to unsaturated polyester resins.¹⁷ Heat flow curves dQ/dt versus time, obtained from the isothermal DSC measurements for samples with 0.5, 1.0, and 2.0 wt % MEKP at different temperatures are shown in Figure 3. As shown, the heat flow values increased with temperature and the initiator concentration, due to increased reaction rate. From the integration of dQ/dt plots, the isothermal heats for each temperature and initiator concentration were calculated. The sum of the isothermal heat and residual heat is the total heat, which was obtained as an average of the values obtained at all temperatures and initiator concentrations. This value was 420 J/g. As a comparison, the heat of homopolymerization for styrene is 701 J/g.¹⁸ The experimental value of 420 J/g indicates that not fully homopolymerization of styrene was accomplished, contrary the copolymer was clearly obtained. Liu et al. have reported the curing of a maleated product obtained from tung oil alcoholysis with pentaerythritol followed by maleinization.¹⁹ They evaluated curing

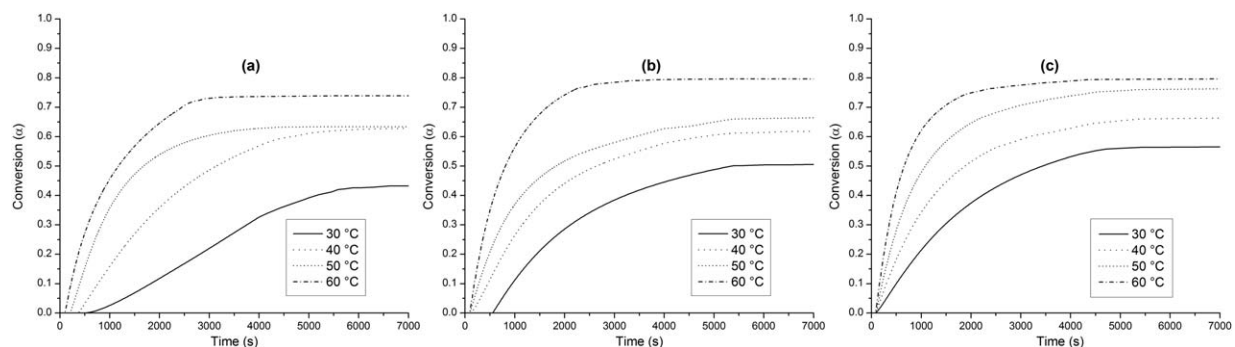


Figure 4. Total conversion versus time for isothermal curing: (a) 0.5 wt % MEKP, (b) 1.0 wt % MEKP, and (c) 2.0 wt % MEKP.

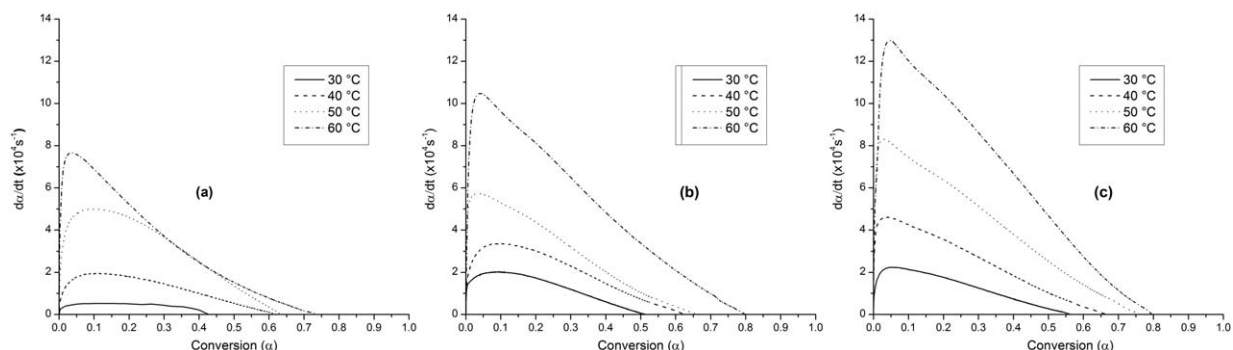


Figure 5. Isothermal conversion rate as a function of conversion: (a) 0.5 wt % MEKP, (b) 1.0 wt % MEKP, and (c) 2.0 wt % MEKP.

of this product with 33% styrene and using *tert*-butyl peroxybenzoate as initiator. Total heat values of reaction ranged from 410–427 J/g, similar to the value obtained in this study. In the case of unsaturated polyester resins cured with styrene, a value of about 231 J/g has been reported.^{20–22}

Overall conversions (α) were calculated from total heat and dQ/dt values at each temperature and initiator concentration applying eq. (2). α values as a function of time are shown in Figure 4. Incomplete cure under isothermal conditions and an increase of conversion with temperature were observed for all initiator concentrations. These are indications of vitrification phenomenon, which occurs when a thermoset is cured at temperatures within the glass transition region of the fully cured resin.²³ Vitrification involves the transformation from a liquid to a glassy state elastomer as a result of the increase in molecular weight.²⁴ Near vitrification, kinetics is affected by the local viscosity, which in turn depends on the degree of reaction and temperature. Therefore, the reaction is stopped before becoming complete due to vitrification, but a temperature increase results in an increase of the reaction rate.²³

Curing rate as a function of conversion for all initiator concentrations and temperatures are shown in Figure 5. It is observed that the curing rate increased with the curing temperature and

the initiator concentration. On the other hand, the maximum values were obtained at conversions lower than 0.2. This indicates a curing process which is very fast at first because of the high availability of monomers. In addition, it is expected that double bonds from maleate groups react faster than those from fatty acid chain. The curing process then becomes slow because the concentration of reactive groups decreases and the viscosity increases due to the increased molecular weight. Formation of polystyrene could have increased curing rate at the beginning of the curing. Delahaye et al. have evaluated the curing of polyester resins with styrene at temperatures between 25 and 65°C, using the system MEKP and cobalt octoate by *in situ* Fourier transform infrared spectroscopy.²⁵ These authors have confirmed that during the curing process the homopolymerization of styrene is faster than the copolymerization of the monomers. Polystyrene formation was confirmed by the peak at 762 cm^{-1} corresponding to C–H stretching ring of polystyrene, in IR analysis (Supporting Information Figure S1).²⁵

From the values obtained for the overall reaction rate, it is possible to calculate certain kinetic parameters as established by several authors.^{26–28} Although during the polymerization process, several simultaneous reactions may occur, empirical models have been developed based on the assumption that only a reaction can represent the entire curing process. In the

Table I. Kinetic Parameters Obtained by eq. (6)

MEKP (wt %)	Temperature (°C)	$k/10^{-3}$ (s^{-1})	m	n	R^2	Standard deviation
0.5	30	0.13	0.29	2.33	0.977	1.6×10^{-6}
	40	1.15	0.52	3.10	0.932	3.3×10^{-5}
	50	2.30	0.44	3.53	0.973	2.2×10^{-4}
	60	1.29	0.13	2.46	0.986	9.0×10^{-5}
1	30	1.2	0.47	4.26	0.972	1.2×10^{-3}
	40	1.3	0.41	3.64	0.991	8.3×10^{-6}
	50	1.4	0.25	3.57	0.989	1.4×10^{-5}
	60	2.1	0.23	2.32	0.985	3.2×10^{-5}
2	30	1.08	0.45	4.20	0.965	5.2×10^{-6}
	40	1.08	0.25	3.20	0.982	1.1×10^{-5}
	50	15.5	0.19	2.48	0.987	2.4×10^{-4}
	60	2.89	0.26	2.42	0.989	3.6×10^{-5}

Table II. Kinetic Parameters Obtained by eq. (7)

MEKP (wt %)	Temperature (°C)	$k_1/10^{-3}$ (s ⁻¹)	$k_2/10^{-3}$ (s ⁻¹)	m	n	R^2	Standard deviation
0.5	30	0.02	0.96	0.96	7.99	0.810	1.4×10^{-4}
	40	0.14	1.4	0.85	3.27	0.977	2.7×10^{-6}
	50	0.23	3.7	0.77	4.01	0.984	2.5×10^{-5}
	60	0.73	2.1	0.97	3.10	0.951	2.7×10^{-5}
1	30	0.15	2.2	0.91	4.90	0.987	8.7×10^{-2}
	40	0.15	2.5	0.80	4.46	0.987	7.4×10^{-6}
	50	0.41	3.0	0.83	4.45	0.978	1.4×10^{-5}
	60	0.26	1.8	0.25	2.26	0.981	1.3×10^{-5}
2	30	0.15	2.0	0.90	4.89	0.972	5.2×10^{-6}
	40	0.36	2.2	0.89	4.01	0.978	1.1×10^{-5}
	50	1.2×10^{-6}	16	0.19	2.48	0.987	2.5×10^{-4}
	60	0.69	4.4	0.70	2.88	0.971	3.1×10^{-5}

absence of diffusional control, the general reaction is described by eq. (4).

$$\frac{d\alpha}{dt} = kf(\alpha) \quad (4)$$

The simplest model corresponds to an n -order kinetic model [eq. (5)].²⁸ This equation does not account for autocatalytic effects and predicts a maximum reaction rate at $t = 0$.

$$\frac{d\alpha}{dt} = k(1-\alpha)^n \quad (5)$$

The eq. (6) has been applied for autocatalytic systems:

$$\frac{d\alpha}{dt} = k\alpha^m(1-\alpha)^n \quad (6)$$

Both n -order as autocatalytic kinetic models use a single kinetic constant for modeling the curing process. In practice, many events can occur simultaneously and lead to a very complex reaction system and consequently the use of multiple rate constants can provide more accurate results. Kamal's model [eq. (7)] involves two rate constants and two orders of reaction (m and n). This model has been widely applied in the literature

to represent the curing of thermoset resins such as epoxy resins and unsaturated polyester.^{28,29}

$$\frac{d\alpha}{dt} = (k_1 + k_2\alpha^m)(1-\alpha)^n \quad (7)$$

In order to take into account the vitrification, these models are modified as shown in eq. (8), where α_{\max} is the maximum conversion reached for each isothermal experiment.³⁰

$$\frac{d\alpha}{dt} = k \left(\frac{\alpha_{\max} - \alpha}{\alpha_{\max}} \right)^x \alpha^m (1-\alpha)^n \quad (8)$$

Kinetic parameters defined by eqs. (6–8) were calculated from overall reaction rate data. A nonlinear multiple regression through a Levenberg-Marquardt algorithm using MATLAB[®] was used.^{29,31} Kinetic parameters obtained for each of the models as well as the corresponding coefficient of determination (R^2) and the standard error of the estimates at various concentrations of initiator and temperatures are reported in Tables (I–III). Experimental values of $d\alpha/dt$ and those calculated from different kinetic models, at 1.0 wt % MEKP, are compared in Figure 6.

Table III. Kinetic Parameters Obtained by eq. (8)

MEKP (wt %)	Temperature (°C)	$k/10^{-3}$ (s ⁻¹)	x	m	n	R^2	Standard deviation
0.5	30	0.89	0.72	0.56	4.23	0.793	4.8×10^{-6}
	40	1.12	0.04	0.47	3.20	0.915	1.2×10^{-4}
	50	1.43	0.55	0.31	1.65	0.999	3.5×10^{-5}
	60	1.56	0.00	0.20	2.71	0.978	2.1×10^{-5}
1	30	0.89	0.48	0.38	2.75	0.989	3.2×10^{-4}
	40	1.52	0.10	0.46	3.67	0.987	5.2×10^{-4}
	50	1.23	0.25	0.22	2.92	0.985	6.6×10^{-6}
	60	2.46	0.01	0.25	2.62	0.972	2.3×10^{-4}
2	30	1.34	0.33	0.52	3.92	0.933	4.6×10^{-4}
	40	1.62	0.27	0.38	3.29	0.947	5.5×10^{-5}
	50	17.01	0.00	0.22	2.61	0.986	7.1×10^{-6}
	60	3.60	0.21	0.30	2.64	0.959	4.3×10^{-5}

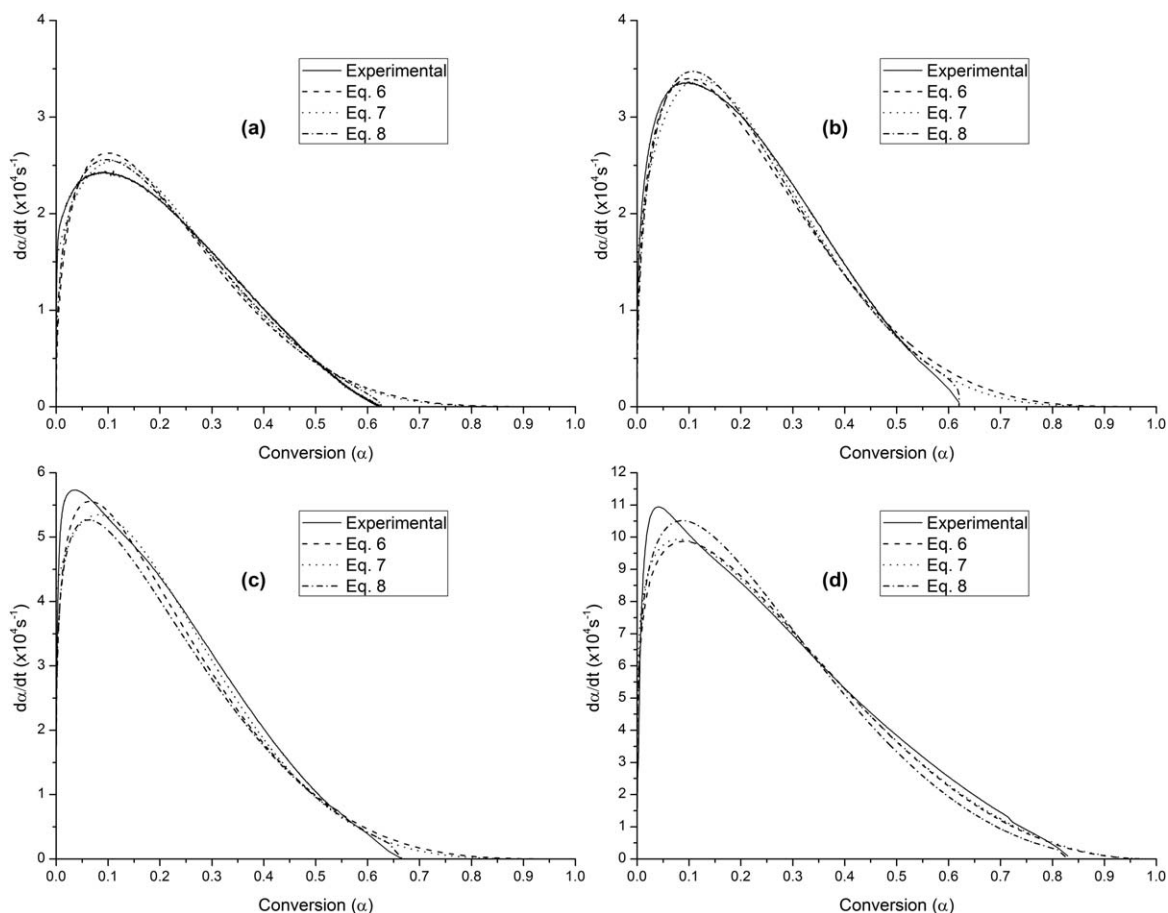


Figure 6. Results obtained with different kinetic models with 1% MEKP: (a) 30°C, (b) 40°C, (c) 50°C, and (d) 60°C.

According to Tables (I–III), with some exceptions, a good fit of the data to the three kinetics models was observed. According to Figure 6 (1% MEKP), at 30 and 40°C, the three models show a good agreement with experimental data at conversions lower than 0.55. At higher conversions, some deviations were observed with the autocatalytic and Kamal's models. The deviations observed at conversions higher than 0.55 can be attributed to vitrification. Indeed the agreement of experimental data with the kinetic model that includes vitrification [eq. (8)] was in

general better over the entire range of conversions in comparison with the other models, at 30–40°C. On the other hand, at high temperatures (50–60°C), deviations were observed predominantly at low and high conversions. Deviations at high reaction rates which makes it impossible collect the initial values for dx/dt . Deviations at high temperature and high conversions were less significant at 60°C with respect to 50°C because vitrification effect diminishes with the temperature.³⁰

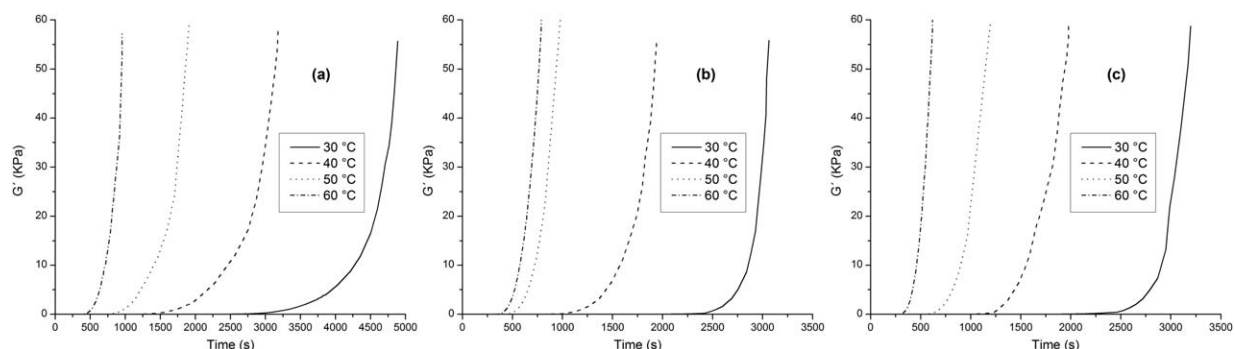


Figure 7. Storage modulus as a function of time: (a) 0.5 wt % MEKP, (b) 1.0 wt % MEKP, and (c) 2.0 wt % MEKP.

Table IV. Gel Times Obtained for Isothermal Curing Reactions

Temperature (°C)	Gel time (s)		
	MEKP (wt %)		
	0.5	1.0	2.0
30	2700	2200	2100
40	1280	1150	1060
50	740	635	565
60	406	364	300

Rheological Characterization

From oscillatory rheological measurements, it is possible to determine the viscoelastic properties, the gel point, and thereof the E_a .¹⁵ The gel point was determined by the intersection of the curves of G' and G'' , at each temperature and initiator concentration, according to ASTM D4473–08 standard. This test method provides a simple means of characterizing the cure behavior of thermosetting resins measuring the elastic and loss moduli as a function of temperature or time, or both. Storage modulus as a function of time at several initiator concentrations are shown in Figure 7. Following the procedure described above, gel times for the whole temperature range and initiator concentrations were determined, as shown in Table IV. It is observed that by increasing the temperature and/or the initiator concentration the gel times decreased because reaction rates increase. For practical purposes, the processing of MACOG-based resins, with cobalt octoate as a catalyst and MEKP as initiator, should be performed at temperatures between 30 and 40°C with initiator concentrations between 0.5 and 1%. It should be noted that the concentration of catalyst used was 0.5%, if it is higher, the gel time could decrease.

Because there is a linear relationship between $\ln(t_g)$ and the inverse of temperature for isothermal curing reactions [eq. (3)], it is possible to calculate E_a values from the slope of this graph. Table V reports the values obtained. The values of E_a values obtained were within the typical range of unsaturated polyester resins cured with redox initiators (40–60 kJ/mol).³² On the other hand, the value of E_a for styrene homopolymerization reported in the literature is 32.5 kJ/mol, which is lower than the obtained for copolymerization with MACOG because styrene is more reactive.³³ E_a values diminished with MEKP concentration indicating that the reaction mechanism changes with the reaction conditions as it was mentioned above during kinetic studies by DSC. This effect has been reported previously for cured unsaturated polyester resins with styrene, and benzoyl peroxide or MEKP as initiators.^{34,35}

Table V. E_a Values Calculated from eq. (3)

MEKP (wt %)	E_a (kJ/mol)
0.5	52.3
1.0	50.3
2.0	47.2

CONCLUSIONS

The kinetics of copolymerization of MACOG obtained from biodiesel-derived crude glycerol and styrene were studied by DSC and rheology. According to the kinetic analysis by DSC, curing rate increases with temperature and initiator concentration. Maximum conversion was 0.81, obtained at 60°C and 2% MEKP. Fitting of experimental curing rates to various models was evaluated. The three models show a good agreement with experimental data at conversions lower than 0.55 and 30–40°C. However, for these temperatures, the model that includes vitrification showed a better agreement in the entire range of conversions. At higher temperatures (50–60°C), some deviations were observed at low and high conversions for the three models. According to the reaction orders obtained from these models, it is concluded that the mechanism of the reaction varies depending on the initiator concentration and temperature.

Gel times, determined by rheology, were 300–2700 s. These values decreased with the temperature and the initiator concentration. For practical purposes, the processing of the developed resins should be performed at temperatures of 30–40°C with initiator concentrations of 0.5–1 wt %. E_a values ranged from 47.2 to 52.3 kJ/mol depending on the concentration of MEKP. These values were within the typical range of unsaturated polyester resins cured with redox initiators. According to DSC and rheology results, copolymerization of MACOG prevails over homopolymerization of styrene.

ACKNOWLEDGMENTS

Financial support of “Departamento Administrativo de Ciencia, Tecnología e Innovación–Colciencias, Convocatoria de Doctorados Nacionales 2008,” “Colciencias–Patrimonio Autónomo Fondo Nacional de Financiamiento para la Ciencia, la Tecnología y la Innovación, Francisco José de Caldas,” and “Universidad de Antioquia, Comité para el Desarrollo de la Investigación–Sostenibilidad 2013–2014” is acknowledged.

REFERENCES

- Biermann, U.; Bornscheuer, U.; Meier, M. A. R.; Metzger, J. O.; Schäfer, H. *J. Angew. Chem. Int. Ed. Engl.* **2011**, *50*, 3854.
- United States Department of Energy. Functionalized vegetable oils for use as polymer building blocks. Available at: www1.eere.energy.gov/function_vegoils_polymer_bldgblocks.pdf (Accessed on January 28, 2014).
- Sharma, V.; Kundu, P. P. *Prog. Polym. Sci.* **2006**, *31*, 983.
- Meier, M. A. R.; Metzger, J. O.; Schubert, U. S. *Chem. Soc. Rev.* **2007**, *36*, 1788.
- Can, E.; Küsefoğlu, S.; Wool, R. P. *J. Appl. Polym. Sci.* **2001**, *81*, 69.
- Can, E.; Küsefoğlu, S.; Wool, R. P. *J. Appl. Polym. Sci.* **2002**, *83*, 972.
- Can, E.; Wool, R. P.; Küsefoğlu, S. *J. Appl. Polym. Sci.* **2006**, *102*, 2433.

8. Can, E.; Wool, R. P.; Küsefoğlu, S. *J. Appl. Polym. Sci.* **2006**, *102*, 1497.
9. Echeverri, D. A.; Perez, W. A.; Rios, L. A. *Ind. Crops. Prod.* **2013**, *49*, 299.
10. Echeverri, D.; Cardeño, F.; Rios, L. *J. Am. Oil Chem. Soc.* **2010**, *88*, 551.
11. Yang, F.; Hanna, M.; Sun, R. *Biotechnol. Biofuels* **2012**, *5*, 13.
12. Halley, P. J.; Mackay, M. E. *Polym. Eng. Sci.* **1996**, *36*, 593.
13. Odian, G. Principles of Polymerization; Wiley: New Jersey, **2004**; p 217.
14. Abadie, M. J. M.; Sakkas, D. *Eur. Polym. J.* **1992**, *28*, 873.
15. Gough, L. J.; Smith, I. T. *J. Appl. Polym. Sci.* **1960**, *3*, 362.
16. Flory, P. J. Principles of Polymer Chemistry; Cornell University Press: New York, **1953**; p 106.
17. Roberts, D. E.; Walton, W. W.; Jessup, R. S. *J. Polym. Sci.* **1947**, *2*, 420.
18. Osman, E. A.; Vakhguel, A.; Sbarski, I.; Mutasher, S. A. *Malays. Polym. J.* **2012**, *7*, 46.
19. Liu, C.; Yang, X.; Cui, J.; Zhou, Y.; Hu, L.; Zhang, M.; Liu, H. *Bioresources* **2012**, *7*, 447.
20. Kubota, H. *J. Appl. Polym. Sci.* **1975**, *19*, 2279.
21. Rojas, A. J.; Borrajo, J.; Williams, R. J. *J. Polym. Eng. Sci.* **1981**, *21*, 1122.
22. Azaar, K.; El Brouzi, A.; Granger, R.; Vergnaud, J. M. *Eur. Polym. J.* **1991**, *27*, 1431.
23. Van Assche, G.; Verdonck, E.; Van Mele, B. *J. Therm. Anal. Calorim.* **2000**, *59*, 305.
24. De La Caba, K.; Guerrero, P.; Eceiza, A.; Mondragón, I. *Polymer* **1996**, *37*, 275.
25. Delahaye, N.; Marais, S.; Saiter, J. M.; Metayer, M. *J. Appl. Polym. Sci.* **1998**, *67*, 695.
26. Kenny, J. M. *J. Appl. Polym. Sci.* **1994**, *51*, 761.
27. Worzakowska, M. *J. Appl. Polym. Sci.* **2006**, *102*, 1870.
28. Yousefi, A.; Lafleur, P. G.; Gauvin, R. *Polym. Compos.* **1997**, *18*, 157.
29. Liang, G.; Chandrashekhara, K. *J. Appl. Polym. Sci.* **2006**, *102*, 3168.
30. Stevenson, J. K. *Polym. Eng. Sci.* **1986**, *26*, 746.
31. Rabearison, N.; Jochum, C.; Grandidier, J. C. *J. Mater. Sci.* **2011**, *46*, 787.
32. Lionetto, F.; Maffezzoli, A. *Materials* **2013**, *6*, 3783.
33. Poorabdollah, M.; Beheshty, M. H.; Atai, M.; Vafayan, M. *Polym. Compos.* **2013**, *34*, 1824.
34. Vilas, J. L.; Laza, J. M.; Garay, M. T.; Rodríguez, M.; León, L. M. *J. Appl. Polym. Sci.* **2001**, *79*, 447.
35. Cuadrado, T. R.; Borrajo, J.; Williams, R. J. J.; Clara, F. M. J. *J. Appl. Polym. Sci.* **1983**, *28*, 485.